A Simple Growth Method to Produce *a*-Plane GaN Thick Films by Hydride Vapor Phase Epitaxy

2013 Jpn. J. Appl. Phys. 52 08JB08

(http://iopscience.iop.org/1347-4065/52/8S/08JB08)

Japanese Journal of Applied Physics **52** (2013) 08JB08 **REGULAR PAPER**
http://dx.doi.org/**10.7567/JJAP.52.08JB08**

A Simple Growth Method to Produce *a*-Plane GaN Thick Films by Hydride Vapor Phase Epitaxy

Yin-Hao Wu, Chuo-Han Lee, Chung-Ming Chu, Yen-Hsien Yeh, Chan-Lin Chen, and Wei-I Lee*

Department of Electrophysics, National Chiao Tung University, Hsinchu 30010, Taiwan
E-mail: wilee@mail.nctu.edu.tw

Received October 11, 2012; accepted November 21, 2012; published online May 20, 2013

A-plane GaN was grown on *r*-plane sapphire using a two-step growth method by hydride vapor phase epitaxy (HVPE). In the first step, *a*-plane GaN formed triangular stripes along the *m*-direction ([$\bar{1}$100] direction) at a low growth temperature. Then, increasing the growth temperature enhanced the lateral growth mode to coalesce *a*-plane GaN in the second step. There were triangular voids formed after growth. In this work, a new method was developed to produce the voids in the *a*-plane GaN film using the two-step growth method without optical lithography.

1. Introduction

Nitride-based materials and devices have attracted much attention owing to their wide applications in optoelectronics and microelectronics, such as visible or ultraviolet light-emitting diodes[1] (LEDs) and laser diodes[2] (LDs). Conventionally, nitride-based devices are grown along the *c*-plane [0001] orientation. These devices suffer strong polarization electrostatic fields along the growth direction. The polarization fields consist of spontaneous and piezoelectric polarization fields. The spontaneous and piezoelectric polarization fields are related to the wurtzite crystal structure and in-plane stress, respectively. These fields lead to the spatial separation of the electrons and holes within the quantum wells. This effect reduces the recombination efficiency in nitride-based devices and the redshift of emission wavelength in optical devices. This phenomenon is called the quantum-confined stark effect[3] (QCSE). To eliminate the polarization field effect, the growth of nonpolar or semipolar planes, such as the *m*-plane[4] ($10\bar{1}0$) and the *a*-plane[5] ($11\bar{2}0$), have been proposed in many research studies. *M*-plane GaN is grown on *m*-plane SiC[6] or β-$LiGaO_2$[7] substrates, and *a*-plane GaN is grown on *r*-plane ($1\bar{1}02$) sapphire.[8] However, the growth of *a*-plane GaN on *r*-plane sapphire is more difficult than that of *c*-plane GaN on *c*-plane sapphire. For example, it is difficult to obtain the smooth surface of *a*-plane GaN grown on *r*-plane sapphire. Another problem is the generation of defects in *a*-plane GaN due to the lattice mismatch between GaN and sapphire. Therefore, there are several methods to improve *a*-plane GaN quality, such as the flow-rate modulation epitaxy technique,[9] epitaxial lateral epitaxial overgrowth[10] (ELOG), and sidewall lateral epitaxial overgrowth[11] (SLEO) techniques.

Blue laser diodes and high-power electric devices are sensitive to the threading dislocation density caused by the lattice mismatch. Furthermore, thermal expansion coefficients are different between GaN and sapphire; thus, there is a possibility that cracks may occur owing to thermal strain. Therefore, homoepitaxy on the *a*-plane GaN substrate is a method of reducing the dislocation density. There are many studies on *c*-direction orientation GaN substrates. GaN substrates can be manufactured by hydride vapor phase epitaxy (HVPE), high-pressure growth, Na flux,[12] and ammonothermal growth methods.[13] *A*-plane GaN films are commonly grown by metal organic vapor phase epitaxy (MOVPE) and in a few cases HVPE.[14,15] The *c*-plane GaN bulks grown by HVPE or ammonothermal method are sliced along the specific facets to produce nonpolar GaN substrates. The size of nonpolar free-standing GaN substrates is too small to manufacture a large number of devices. Nonpolar GaN thick films are grown using the ELOG or SLEO method by HVPE, which is another way of producing nonpolar GaN substrates. However, the lithography process must be used to produce a pattern on sapphire for ELOG. In this paper, we describe the preparation of *a*-plane GaN thick films on *r*-sapphire grown by HVPE. The result obtained without lithography was similar to those obtained using the ELGO method. Then, we discuss the quality and morphology of *a*-plane GaN.

2. Experimental Procedure

A 2-μm-thick *a*-plane GaN layer was initially grown on *r*-plane sapphire by MOCVD as the *a*-plane GaN template.[16] Trimethylgallium (TMGa), trimethyaluminum (TMAl), and ammonia (NH_3) were respectively used as Ga, Al, and N sources in the MOCVD system. The AlN multilayer structure was used as the buffer layer of the *a*-plane GaN template. The AlN multilayer consisted of high-temperature-deposited AlN (HT-AlN), low-temperature-deposited AlN (LT-AlN), and high-temperature-deposited AlN (HT-AlN) from bottom to top. These AlN layers were named as HLH-AlN buffer layers. The growth temperatures of HT-AlN and LT-AlN were 1000 and 800 °C, respectively. Nitrogen was used as the carrier gas during the growth of the AlN buffer layers. Finally, 2-μm-thick *a*-plane GaN films were grown on the multilayer AlN buffer structure by MOCVD, and hydrogen was used as the carrier gas.

An *a*-plane GaN thick film was then grown on an *a*-plane GaN template by HVPE. In the HVPE system, the sources of N and Ga were NH_3 and GaCl, respectively. GaCl was formed with liquid gallium and HCl gas. In this work, the *a*-plane GaN thick film was grown using the two-step growth method by HVPE. In the first step, the growth temperature and pressure were 1000 °C and 100 mbar, respectively. In the second step, the growth temperature was increased to 1050 °C, and the growth pressure was maintained at 100 mbar. Hydrogen was used as the carrier gas in this work. The surface, plane-view, and cross-sectional morphologies of the *a*-plane GaN thick film grown by HVPE were

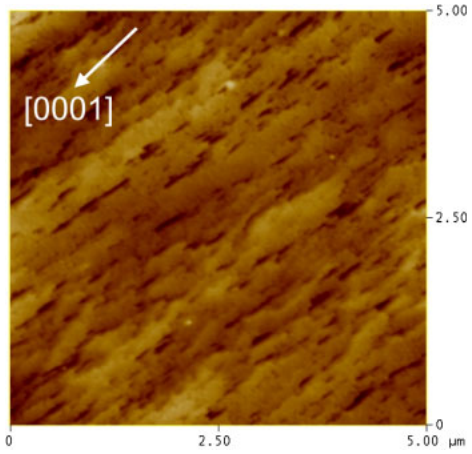

Fig. 1. (Color online) AFM image of *a*-plane GaN template surface grown by MOCVD.

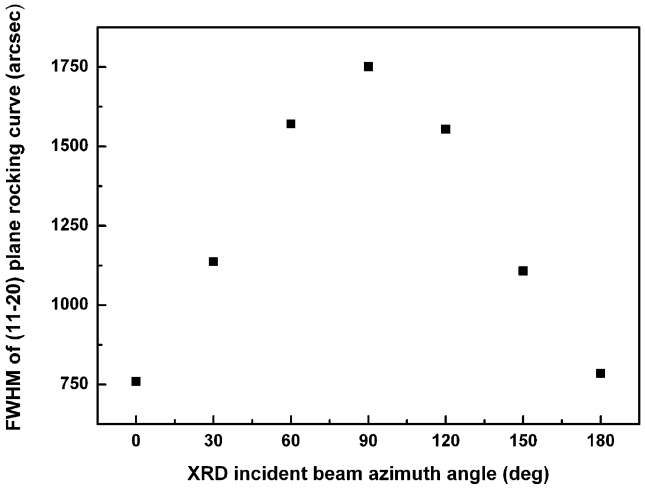

Fig. 2. FWHM of the XRD ($11\bar{2}0$) rocking curve as a function of azimuth angles.

observed by scanning electronic microscopy (SEM). The crystal quality of the *a*-plane GaN thick film was analyzed by high-resolution X-ray diffraction (HRXRD).

3. Results and Discussion

The growth morphology of the *a*-plane GaN template grown by MOCVD was observed by AFM, as shown in Fig. 1. The AFM image reveals the *a*-plane GaN stripes along the GaN *c*-direction ([0001] direction) on the surface. The AFM root mean square (RMS) roughness for $5 \times 5\,\mu m^2$ scanning areas was 1.49 nm. The properties of the *a*-plane GaN template were investigated by HRXRD. Omega rocking curves were measured for the ($11\bar{2}0$) plane reflections to characterize the crystal quality of the *a*-plane GaN template. Figure 2 shows the values of HRXRD omega rocking curves at azimuth angles of 0, 30, 60, 90, 120, 150, and 180° for the *a*-plane GaN template. The XRD incident beam was parallel to the *c*-direction, which was defined as the azimuth angle of 0°, and the sample rotated clockwise to change the azimuth angle. The full width at half maxima (FWHM) was ~750 arcsec when the azimuth angles were 0 and 180°. The maximum FWHM of the azimuth angle was 90°, which

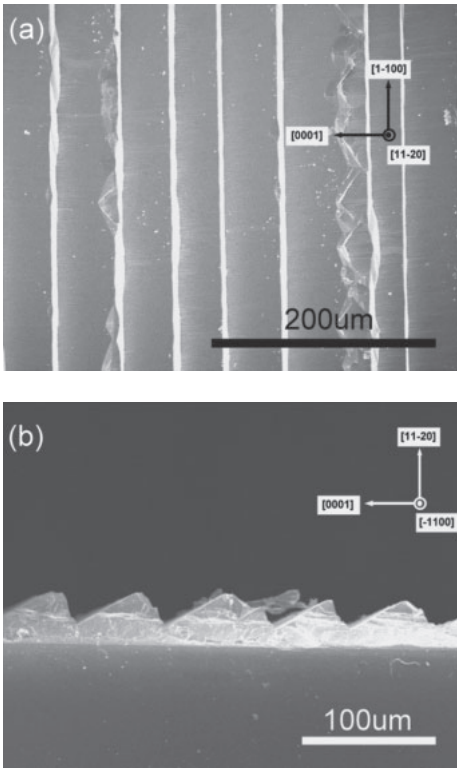

Fig. 3. The SEM images of *a*-plane GaN after the first-step growth: (a) plane-view and (b) cross-sectional image.

indicated that the XRD incident beam was parallel to the *m*-direction. The reason for this rocking curve anisotropy of *a*-plane GaN is currently not clarified. The results suggest the lattice mismatch between *a*-plane GaN and *r*-plane GaN. Additionally, the anisotropic in-plane growth rate is the other factor.[17] The coalescence along the *c*-direction is more than that along the *m*-direction. Thus, the values of the omega rocking curves showed different in-plane anisotropies.

Figures 3(a) and 3(b) reveal the plane-view and cross-sectional SEM images of the first-step growth *a*-plane GaN, respectively. The first-step growth of *a*-plane GaN was carried out at a temperature of 1000 °C and a pressure of 100 mbar by HVPE. The vertical growth rate in the first step was approximately 120 μm/h. There were a large number of obvious stripes along the *m*-direction on the surface. The result of the stripe direction was different from the previous one in this work of the *a*-plane GaN template grown on *r*-plane sapphire. The cross-sectional plane of the stripes along the *m*-direction was triangular. The slopes of the two sides of the triangular plane were obviously different. It was not an isosceles triangle. The slope toward the [0001] direction was smaller than that toward the [000$\bar{1}$] direction. This result suggests that the growth rates of the Ga face (0001) and the N face (000$\bar{1}$) were different. Haskell et al. indicated that the Ga-face sidewall growth was faster than the N face sidewall growth,[18] which was observed using the lateral epitaxial overgrowth (LEO) method.

The specific crystallographic planes toward the Ga face in the stripes, which were the {11$\bar{2}$2} planes, were exposed. Hiramatsu et al. reported that the morphology of *c*-plane GaN was observed using the LEO method under different

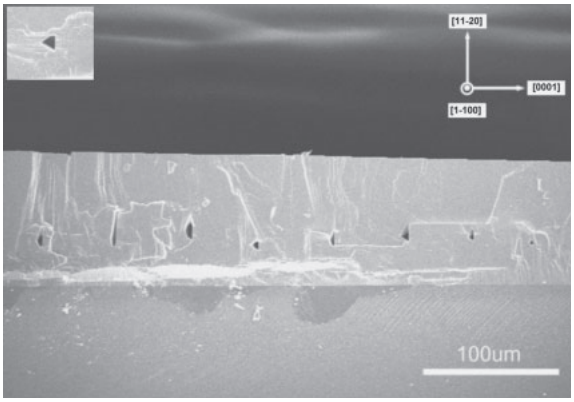

Fig. 4. Cross-sectional SEM image of *a*-plane GaN after the second-step growth. The inset shows the void in the *a*-plane GaN film.

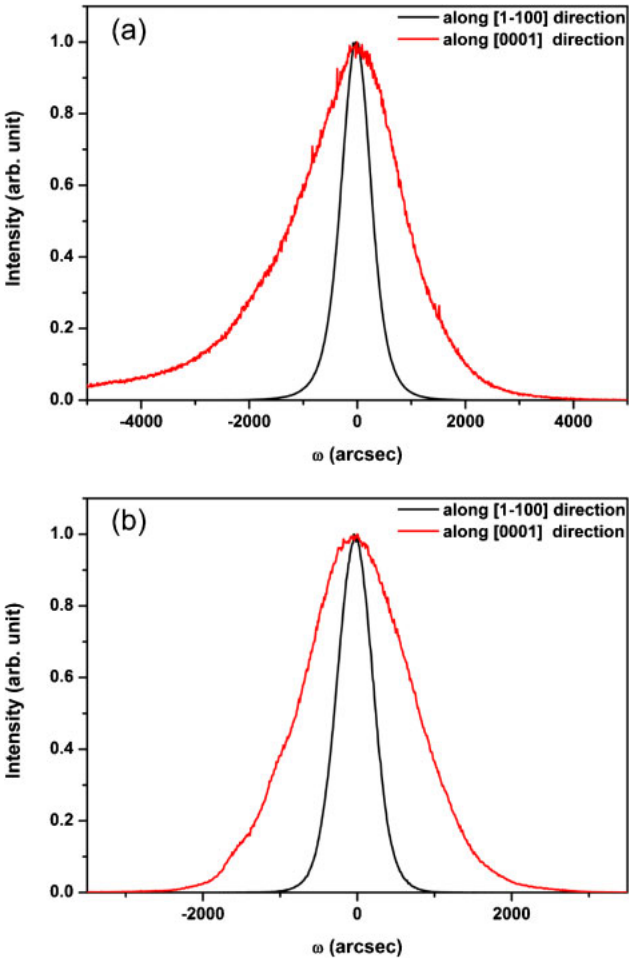

Fig. 5. (Color online) Rocking curves along [0001] and [1$\bar{1}$00] directions (a) after the first-step and (b) second-step growths.

growth conditions by MOCVD.[19] It revealed that the {11$\bar{2}$2} GaN planes on the stripe along the *m*-direction were exposed to a lower growth temperature and a higher growth pressure, which were similar to those presented in this work. The two main factors of the result are considered to be the surface energy and the stability of surface atoms. The {11$\bar{2}$2} facets have N-polarity or Ga-polarity on the surface. N-polarity exposes nitrogen atoms on the surface, which are stable at a low growth temperature.[19] Thus, we considered that the exposed {11$\bar{2}$2} planes were more stable than the {11$\bar{2}$0} planes under growth conditions in HVPE. Owing to the formation of the stable {11$\bar{2}$2} planes, the stable plane was suppressed to form the (0001) facet. The lateral growth along the *m*-direction was faster than that along the *c*-direction. As shown in Fig. 3(a), the {1$\bar{1}$00} planes coalesced completely and formed triangular stripes along the *m*-direction.

To coalesce and obtain a smooth surface, lateral growth was enhanced. The growth temperature was increased to 1050 °C and the growth pressure was maintained at 100 mbar in the second-step growth. The vertical growth rate in the second step was approximately 30 μm/h, which was lower than that in the first step. Figure 4 shows the cross-sectional SEM image of the *a*-plane GaN thick film along the *m*-direction after the second-step growth. There were many triangular voids formed in the *a*-plane GaN film. These triangular voids were similar to those using the sidewall lateral epitaxial growth method.[11,20] There are two reasons for forming these triangular voids in the films. One is the absence of precursor species at the bottom of the *m*-direction stripes formed in the first-step growth, and the other is the difference in growth rate between the Ga and N faces. The height difference between the high and low stripes formed in the first step was ~20 um. The height hindered the precursor species from arriving at the bottom sufficiently, which suppressed growth from the {11$\bar{2}$2} facet to the (0001) facet. This phenomenon also reveals, in some research studies, the growth of *a*-plane GaN using the LEO and SLEO methods.[11] Ga-face growth rate is usually higher than N-face growth rate, and growth temperature is an important factor for the different growth rates of the Ga and N faces, taking into consideration the different adsorption and desorption rates of the Ga and N faces. Therefore, the Ga-face sidewall coalesced with the N face sidewall in the lateral growth mode and the N-face formed a straight sidewall. The high dangling bond per unit area of facets is unstable at a higher growth temperature and a lower growth pressure. The dangling bond per unit area for the {11$\bar{2}$2} facet is higher than that for the {11$\bar{2}$0} facets. Therefore, we used this property to expose the {11$\bar{2}$0} facets on the top surface, and the Ga-face sidewall exposed the (0001) plane to coalesce with the N-face straight sidewall. Finally, the *a*-plane GaN surface became smooth and the thickness was 100 μm.

The structural quality of the *a*-plane GaN thick films was also characterized by HRXRD. The FWHMs of different rocking curves along the *c*- and *m*-directions were measured, as shown in Fig. 5 (color online). The FWHMs measured along the *c*- and *m*-directions of the first-step growth were 2118 and 647 arcsec, respectively. These FWHMs of the rocking curves along the *c*- and *m*-directions were in contrast to that of the *a*-plane GaN template grown by MOCVD, which suggests that the surface along the *c*-direction did not coalesce completely, causing a rough surface. Thus, the FWHM of the rocking curve along the *m*-direction was smaller than that along the *c*-direction. The FWHMs measured along the *c*- and *m*-directions of the second-step growth were 1410 and 427 arcsec, respectively. Owing to the coalescence of the surface and the increase in thickness, the crystal quality was improved. Although the FWHMs

measured along the two directions decreased, the FWHM of the rocking curve along the *m*-direction was still smaller than that along the *c*-direction. This was attributed to the bowling radius difference between the *c*- and *m*-directions. The bowling radius was estimated using the formula $R = \Delta X/(\omega_1 - \omega_2)$ with the HRXRD rocking curve (002) ω-scan. ΔX is the distance of two points of X-ray incidence. The two X-ray incident angles differ owing to the bowling effect. Thus, ω_1 and ω_2 are the diffraction angles with respect to ΔX.[21] The bowling radii of the *c*- and *m*-directions of *a*-plane GaN were estimated to be 65 and 40 cm, respectively. Both the *c*- and *m*-directions of curvature were convex. Therefore, the bowling effect of the *c*-direction was more obvious than that of the *m*-direction, which affected the crystal quality.

4. Conclusions

In conclusion, a nonpolar $(11\bar{2}0)$ *a*-plane GaN film was grown by HVPE using a two-step growth method. In the first step, the triangular stripes of GaN along $[1\bar{1}00]$ formed and exposed the $\{11\bar{2}2\}$ facet to a low growth temperature. In the second step, the lateral growth mode was enhanced, exposing the $\{11\bar{2}0\}$ facet by increasing the growth temperature. Triangular voids can were formed in *a*-plane GaN films using the two-step growth method. These voids were similar to those employed by SELO without lithography. The crystal quality of the *a*-plane GaN film was improved by the two-step growth method.

1) S. Nakamura and T. Mukai: Jpn. J. Appl. Phys. **30** (1991) L1998.
2) S. Nakamura: Mater. Sci. Eng. B **59** (1999) 370.
3) D. A. B. Miller, D. S. Chemla, T. C. Damen, A. C. Gossard, W. Wiegmann, T. H. Wood, and C. A. Burrus: Phys. Rev. Lett. **53** (1984) 2173.
4) C. Wetzel, M. Zhu, J. Senawiratne, T. Detchprohm, P. D. Persans, L. Liu, E. Preble, and D. Hanser: J. Cryst. Growth **310** (2008) 3987.
5) A. Chitnis, C. Chen, V. Adivarahan, M. Shatalov, E. Kuokstis, V. Mandavilli, J. Yang, and M. A. Khan: Appl. Phys. Lett. **84** (2004) 3663.
6) B. Imer, F. Wu, M. D. Craven, J. S. Speck, and S. P. DenBaars: Jpn. J. Appl. Phys. **45** (2006) 8644.
7) M. M. C. Chou, C. Chen, D. R. Hang, and W. T. Yang: Thin Solid Films **519** (2011) 5066.
8) M. D. Craven, S. H. Lim, F. Wu, J. S. Speck, and S. P. DenBaars: Appl. Phys. Lett. **81** (2002) 469.
9) J. J. Huang, T. Y. Tang, C. F. Huang, and C. C. Yang: J. Cryst. Growth **310** (2008) 2712.
10) M. D. Craven, S. H. Lim, F. Wu, J. S. Speck, and S. P. DenBaars: Appl. Phys. Lett. **81** (2002) 1201.
11) B. M. Imer, F. Wu, S. P. DenBaars, and J. S. Speck: Appl. Phys. Lett. **88** (2006) 061908.
12) F. Kawamura, M. Morishita, M. Tanpo, M. Imade, M. Yoshimura, Y. Kitaoka, Y. Mori, and T. Sasaki: J. Cryst. Growth **310** (2008) 3946.
13) R. Dwiliński, R. Doradziński, J. Garczyński, L. P. Sierzputowski, A. Puchalski, Y. Kanbara, K. Yagi, H. Minakuchi, and H. Hayashi: J. Cryst. Growth **310** (2008) 3911.
14) T. Paskova, V. Darakchieva, P. P. Paskov, J. Birch, E. Valcheva, P. O. A. Persson, B. Arnaudov, S. Tungasmitta, and B. Monemar: J. Cryst. Growth **281** (2005) 55.
15) T. Paskova, P. P. Paskov, E. Valcheva, V. Darakchieva, J. Birch, A. Kasic, B. Arnaudov, S. Tungasmita, and B. Monemar: Phys. Status Solidi A **201** (2004) 2265.
16) C. H. Chiang, K. M. Chen, Y. H. Wu, Y. S. Yeh, W. I. Lee, J. F. Chen, K. L. Lin, Y. L. Hsiao, W. C. Huang, and E. Y. Chang: Appl. Surf. Sci. **257** (2011) 2415.
17) H. Wang, C. Chen, Z. Gong, J. Zhang, M. Gaevski, M. Su, J. Yang, and M. A. Khan: Appl. Phys. Lett. **84** (2004) 499.
18) B. A. Haskell, F. Wu, M. D. Craven, S. Matsuda, P. T. Fini, T. Fujii, K. Fujito, S. P. DenBaars, J. S. Speck, and S. Nakamura: Appl. Phys. Lett. **83** (2003) 644.
19) K. Hiramatsu, K. Nishiyama, A. Motogaito, H. Miyake, Y. Iyechika, and T. Maeda: Phys. Status Solidi A **176** (1999) 535.
20) B. Imer, F. Wu, J. Speck, and S. Denbaars: J. Cryst. Growth **306** (2007) 330.
21) S. H. Park, J. H. Chang, D. C. Oh, T. Minegishi, W. H. Lee, H. Goto, H. Suzuki, G. Fujimoto, T. Hanada, and T. Yao: J. Korean Phys. Soc. **49** (2006) 934.